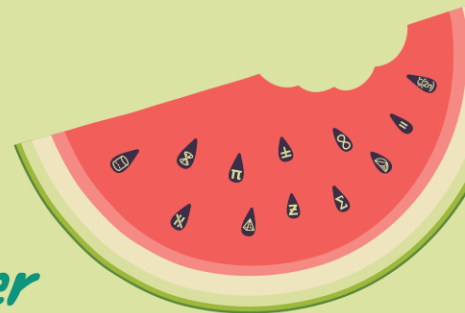


AMSI **SUMMERRESEARCH**
SCHOLARSHIPS 2024–25

Get a taste for Research this Summer



Analytically Predicting the Size of Magnetic Skyrmions in Bulk Materials

Jack Humphreys

Supervised by A/Prof Karen Livesey

University of Newcastle

February 28, 2025

Abstract

Magnetic skyrmions are stable magnetisation textures that have potential applications in improving our data storage technology. An analytic expression for the energy of a skyrmion in a bulk material was found by considering the DMI, anisotropy, demagnetising, exchange and Zeeman energy density contributions. To find an analytic expression and to simplify the calculations, the skyrmion radius was assumed to be significantly larger than the wall width. The total energy was then minimised to find the favourable helicity, radius, and wall width.

1 Introduction

A magnetic skyrmion is a stable magnetisation texture found within magnetic materials. A picture of one is given in Fig. 1, with the arrows showing the direction of the local magnetisation. The magnetisation arrows inside its circular core (blue arrows into the page) are in the opposite direction to the magnetisation outside (red arrows out of the page).

The way in which the magnetisation rotates from up to down from the skyrmion core to outside can vary and is known as its *helicity*. In Fig. 1, the skyrmion has a “whirlpool” shape with the magnetization pointing along the azimuthal direction in the transition or wall region of the skyrmion. Another helicity would be for magnetization in the wall region to point radially outwards.

Skyrmions could be utilised in future data storage technology that is lower energy and higher density than our existing technology (Tomasello et al. 2014). To build future technology with skyrmions, we must better our understanding of their behaviour and features. The characteristics of skyrmions have been measured experimentally and calculated numerically, but there are few analytic equations that describe their geometry. Such an equation is useful as it can be used to predict skyrmion features for any given magnetic material and for external parameters such as applied magnetic field strength. An analytic equation describing the radius and wall width of skyrmions in thin films has been found (Lu et al. 2023), but there are few equivalent equations for skyrmions in bulk materials.

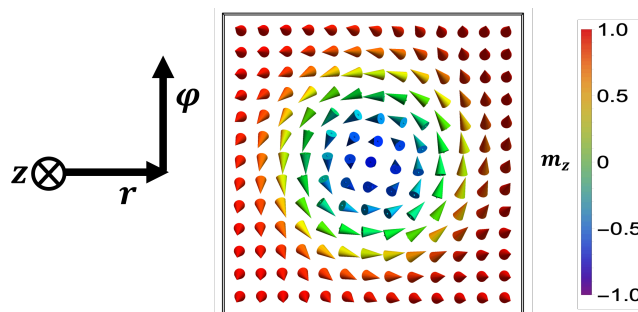


Figure 1: A top-down view of a Bloch type skyrmion in the x - y plane, showing the radial dependence of the out-of-plane magnetisation component, m_z .

In this report, we characterise skyrmions in bulk materials by predicting their radius, wall width and helicity using an analytic equation. This is done by extending the method used by Lu et al. (2023), which is an energy minimisation technique. The total skyrmion energy is found by considering the relevant energy contributions from magnetic phenomena. One such notable contribution is the *Dzyaloshinskii-Moriya interaction* (DMI), which is responsible for stabilising skyrmions by favouring rotation in the magnetisation.

Statement of Authorship

All derivations presented in this report have been developed by the author, Jack Humphreys, based on ideas developed by A/Prof Karen Livesey. The author acknowledges this project follows the methods used by Ellen Lu, a previous AMSI scholar supervised by A/Prof Livesey.

2 Definitions

Before discussing and deriving the magnetic energy contributions of a skyrmion, we detail expressions for the magnetisation of a skyrmion, which has cylindrical symmetry. Some useful expressions will also be derived, which are needed before moving to Sec. 3.

2.1 Magnetisation Vector

The magnetisation is assumed to vary only in the radial direction and so can be defined as a unit vector using cylindrical coordinates

$$\hat{\mathbf{m}}(r) = \underbrace{\cos \Phi \sin \theta(r)}_{m_r} \hat{\mathbf{r}} + \underbrace{\sin \Phi \sin \theta(r)}_{m_\varphi} \hat{\boldsymbol{\varphi}} + \underbrace{\cos \theta(r)}_{m_z} \hat{\mathbf{z}}, \quad (1)$$

where the polar angle of the magnetisation profile, θ , only varies in the radial direction, and where the helicity of the skyrmion, Φ , is constant and defined in the range $-\pi < \Phi \leq \pi$. The cylindrical coordinate system is drawn on the skyrmion picture in Fig. 1.

If $\Phi = 0$ or π , then $m_\varphi = 0$ and the magnetisation only rotates in the radial direction given by $m_r = \pm \sin \theta(r)$. This creates a ‘hedgehog’ rotation known as a Néel-type skyrmion. The different signs of m_r represent two opposite chiralities.

Conversely, if $\Phi = \pm \frac{\pi}{2}$, then $m_r = 0$ and the magnetisation only rotates in the azimuthal direction given by $m_\varphi = \pm \sin \theta(r)$. This creates a ‘whirlpool’ rotation known as a Bloch-type skyrmion. Again, the different signs of m_φ represent two opposite chiralities.

In this project, we aim to find both the helicity Φ and the profile $\theta(r)$ for a skyrmion in a given magnetic material.

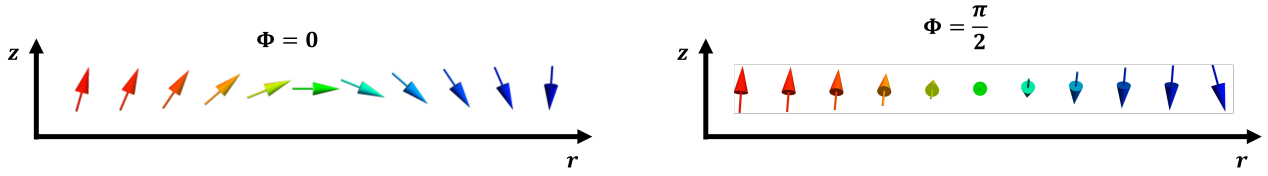


Figure 2: A slice of the r - z plane showing the radial rotation in Néel (left) and azimuthal rotation in Bloch (right) skyrmions

2.2 Magnetisation Profile, $\theta(r)$

An ansatz is used for the magnetisation profile. Namely, the polar angle is given by

$$\theta(r) = 2 \arctan \left(\frac{\sinh \left(\frac{r}{w} \right)}{\sinh \left(\frac{R}{w} \right)} \right), \quad (2)$$

where R is the skyrmion radius, and w is the wall width. This represents the magnetisation pointing in the positive z -direction within the core of the skyrmion. The skyrmion radius is defined as the distance from the center of the core to the edge ($m_z = 0$).

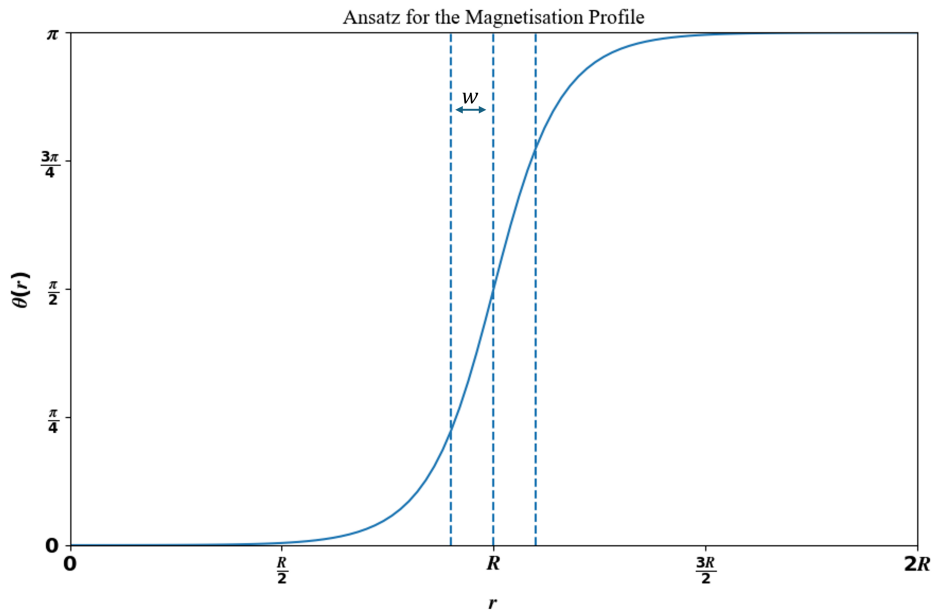


Figure 3: A plot of the magnetisation profile, $\theta(r)$, varying with radius, r .

This ansatz is useful for finding analytical solutions and has been used in previous studies on skyrmion size (Wang et al. 2018). Essentially, the problem will be reduced to finding the constants R , w and Φ which minimize the total skyrmion energy.

Using a t-result substitution where

$$t = \tan \left(\frac{\theta}{2} \right) = \frac{\sinh \left(\frac{r}{w} \right)}{\sinh \left(\frac{R}{w} \right)},$$

a simplified form for the out-of-plane magnetisation component m_z can be found

$$\begin{aligned}
 m_z(r) &= \cos \theta(r) \\
 &= \frac{1 - t^2}{1 + t^2} \\
 &= \frac{\sinh\left(\frac{R+r}{w}\right) \sinh\left(\frac{R-r}{w}\right)}{\cosh\left(\frac{R+r}{w}\right) \cosh\left(\frac{R-r}{w}\right) - 1} \\
 &\approx \frac{\sinh\left(\frac{R+r}{w}\right) \sinh\left(\frac{R-r}{w}\right)}{\cosh\left(\frac{R+r}{w}\right) \cosh\left(\frac{R-r}{w}\right)} \quad (\text{when } R \gg w) \\
 &= \tanh\left(\frac{R+r}{w}\right) \tanh\left(\frac{R-r}{w}\right) \\
 &\approx \tanh\left(\frac{R-r}{w}\right) \quad (\text{for } r \geq 0 \text{ when } R \gg w) \\
 \therefore \cos \theta(r) &\approx \tanh\left(\frac{R-r}{w}\right). \quad (3)
 \end{aligned}$$

This approximation assumes the skyrmion radius is significantly larger than the wall width, which will be assumed throughout each calculation. The accuracy of these expressions compared to the exact forms is shown in Fig. 4.

Using the Pythagorean trigonometric and equivalent hyperbolic identities, the in-plane component of the magnetisation is given by

$$\sin \theta(r) \approx \operatorname{sech}\left(\frac{R-r}{w}\right). \quad (4)$$

The gradient of the polar angle $\theta'(r)$ will also be required in our subsequent derivations of the skyrmion energy contributions, in Sec. 3. By differentiating (3) implicitly, and then substituting (4), it is found to be

$$\theta'(r) \approx \frac{1}{w} \cdot \operatorname{sech}\left(\frac{R-r}{w}\right). \quad (5)$$

3 Energy Contributions

The total energy of a skyrmion can be expressed as the sum of the DMI, anisotropy, exchange, demagnetizing and Zeeman energies, namely

$$E_{total} = E_{DMI} + E_{anis} + E_{ex} + E_d + E_{zee}.$$

These contributions will be described in more detail in the following subsections. Each energy contribution can be found by integrating the corresponding energy density, U , across the magnetic material's volume v according to

$$\begin{aligned}
 E &= \int_v U \, dv \\
 &= \int_0^t \int_0^{2\pi} \int_0^\infty U(r) \cdot r \, dr \, d\varphi \, dz \\
 &= 2\pi t \int_0^\infty r \cdot U(r) \, dr. \quad (6)
 \end{aligned}$$

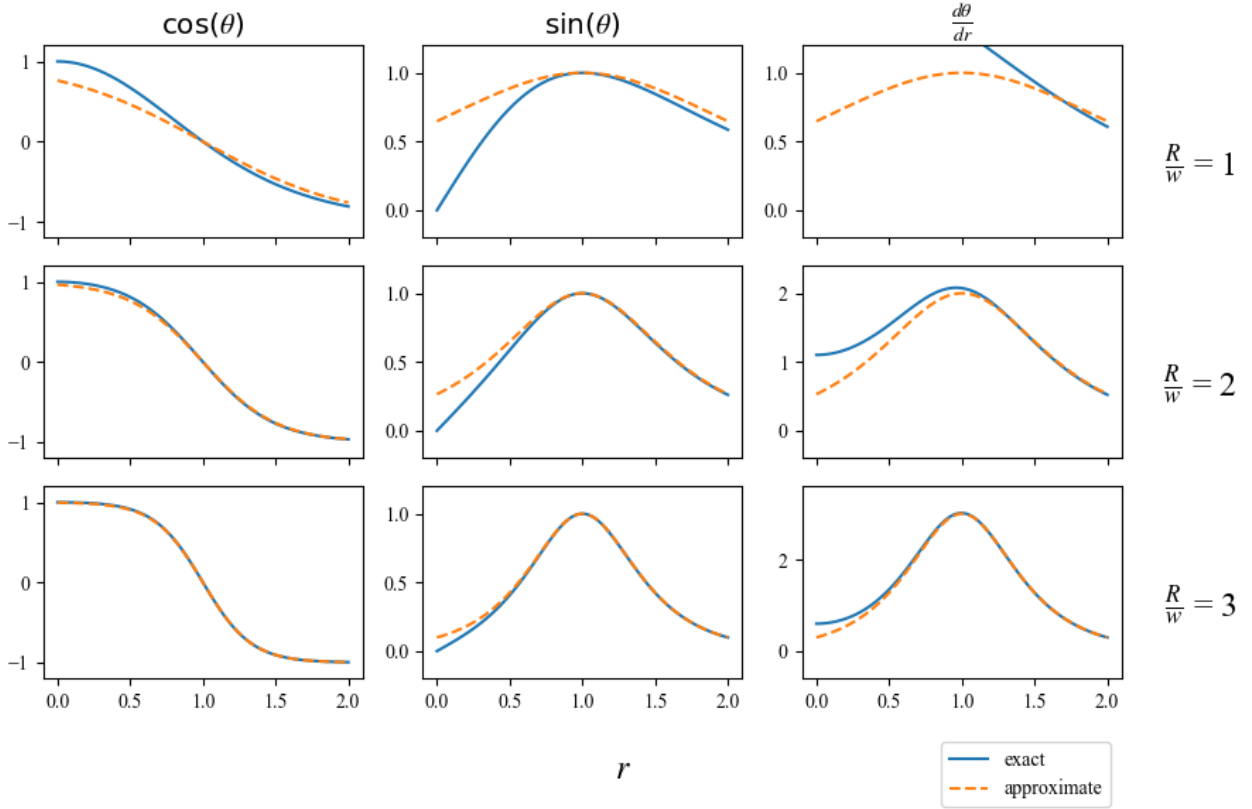


Figure 4: Comparisons between the exact and approximate expressions for the out-of-plane magnetisation component (left), the in-plane magnetisation component (middle), and the gradient of the polar angle (right), for varying ratios of $\frac{R}{w}$.

3.1 DMI

The Dzyaloshinskii-Moriya interaction (DMI) is a quantum-mechanical interaction between neighbouring magnetic moments inside a material. As mentioned in the introduction, DMI favours the rotation of magnetisation and is therefore important for the existence of magnetic skyrmions (Camley & Livesey 2023). The energy density of the DMI in bulk materials is given in Cartesian coordinates by

$$U_{DMI}^{bulk} = D \left(m_y \frac{\partial m_z}{\partial x} - m_z \frac{\partial m_y}{\partial x} + m_z \frac{\partial m_x}{\partial y} - m_x \frac{\partial m_z}{\partial y} + m_x \frac{\partial m_y}{\partial z} - m_y \frac{\partial m_x}{\partial z} \right), \quad (7)$$

where D is the strength of the atomic DMI vector (Camley & Livesey 2023). This expression was converted to cylindrical coordinates, assuming that there is no variation in the magnetisation in either the z or φ directions. The result is

$$U_{DMI}^{bulk} = D \left(m_\varphi \frac{\partial m_z}{\partial r} - m_z \frac{\partial m_\varphi}{\partial r} - \frac{m_z m_\varphi}{r} \right). \quad (8)$$

Substituting the components from Eq. (1) with the ansatz approximations Eqs. (3), (4) & (5) into this DMI energy density expression Eq. (8) leads to

$$U_{DMI}^{bulk} = -D \sin \Phi \left(\theta'(r) + \frac{\sin \theta(r) \cos \theta(r)}{r} \right) \\ \approx -D \sin \Phi \left(\frac{1}{w} \cdot \operatorname{sech} \left(\frac{R-r}{w} \right) + \frac{\operatorname{sech} \left(\frac{R-r}{w} \right) \tanh \left(\frac{R-r}{w} \right)}{r} \right). \quad (9)$$

This simplified expression for the DMI energy density using the magnetisation profile ansatz enables the energy contribution due to DMI to be derived analytically by substituting Eq. (9) into Eq. (6). Namely,

$$E_{DMI} = 2\pi t \times (-D \sin \Phi) \int_0^\infty \left(\frac{r}{w} \operatorname{sech} \left(\frac{R-r}{w} \right) + \operatorname{sech} \left(\frac{R-r}{w} \right) \tanh \left(\frac{R-r}{w} \right) \right) dr \\ \approx 2\pi t \times (-D \sin \Phi) \int_0^\infty \frac{R}{w} \operatorname{sech} \left(\frac{R-r}{w} \right) dr - 2\pi t \times D \sin \Phi \int_{\frac{R}{w}}^{-\infty} \operatorname{sech}(\rho) \tanh(\rho) \cdot (-w) d\rho \\ \text{(For } R \gg w) \\ \approx 2\pi t \times (-D \sin \Phi) \times (-R) \left[\arctan \left(\sinh \left(\frac{R-r}{w} \right) \right) \right]_0^\infty - 2\pi t \times D \sin \Phi \int_\infty^{-\infty} \operatorname{sech}(\rho) \tanh(\rho) \cdot (-w) d\rho \\ \text{(For } R \gg w) \\ = 2\pi t \times (-D \sin \Phi) \times (-R) \left[\arctan(-\infty) - \arctan \left(\sinh \left(\frac{R}{w} \right) \right) \right]_0^\infty - 2\pi t \times D \sin \Phi \times 0 \\ \text{(Odd function)} \\ \approx 2\pi t \times (-D \sin \Phi) \times R \left(\frac{\pi}{2} + \frac{\pi}{2} \right) \\ \text{(For } R \gg w) \\ = 2\pi t \times (-D \sin \Phi) \times \pi R. \quad (10)$$

The DMI inherently favours chiral structures. One sees that this energy contribution is reduced if the chirality $\Phi = \pi/2$ (Bloch skyrmion). The magnetisation rotation occurs in the wall of the skyrmion (the transition from up to down), which has a total length of $2\pi R$. Eq. (10) validates this prediction as the energy indeed scales as $2\pi R$.

We note that the bulk DMI energy found here matches the result by Wang et al. (2018). It is also of the same form as the DMI energy in thin film magnets, apart from $\sin \Phi$ replacing $\cos \Phi$ (Lu et al. 2023). The replacement of \sin by \cos reflects that Bloch skyrmions are found in bulk materials while Néel skyrmions – with opposite chirality Φ – are found in magnetic thin films with DMI.

3.2 Anisotropy

Anisotropy describes the energy cost when the local magnetisation is misaligned from a preferred axis. Here, the preferred axis is in the z direction, meaning magnetisation in the skyrmion core and outside the skyrmion reduces this energy contribution. Skyrmions, that involve gradual changes in the magnetisation away from the out-of-plane axis, inherently have an anisotropy energy cost. The anisotropy energy density that favours alignment in the z direction is given by (Aharoni 2000)

$$U_{anis} = K(1 - m_z^2), \quad (11)$$

where K is the anisotropy constant for a particular magnetic material with units of J/m^3 . This expression can be substituted into our energy integral, Eq. (6), to give

$$\begin{aligned} E_{anis} &= 2\pi t \times K \int_0^\infty r \operatorname{sech}^2\left(\frac{R-r}{w}\right) dr \\ &\approx 2\pi t \times K \int_0^\infty R \operatorname{sech}^2\left(\frac{R-r}{w}\right) dr && \text{(for } R \gg w\text{)} \\ &= 2\pi t \times KRw \left(1 + \tanh\left(\frac{R}{w}\right)\right) \\ &\approx 2\pi t \times 2KRw. && \text{(for } R \gg w\text{)} \end{aligned}$$

This result predicts that the anisotropy energy increases as the skyrmion grows in size. This is because the region with magnetisation misaligned from the preferred axis grows. Consequently, anisotropy energy favours small skyrmions.

3.3 Demagnetising Energy

Magnets have an internal magnetic field, which interacts with the internal magnetization \vec{m} . Maxwell's equations govern this internal magnetic field, which is also known as a ‘‘demagnetising field’’ H_d . Assuming the skyrmion varies only in the radial direction, the simplified expression for demagnetising energy density arising from the demagnetising field is (van Dijk 2015)

$$U_d(r) = -\frac{\mu_0}{2} M_s \vec{m}(r) \cdot \vec{H}_d(r) = \frac{\mu_0}{2} M_s^2 m_r^2, \quad (12)$$

where μ_0 is the magnetic permeability of free space and M_s is the magnetic saturation of a given material. SI units are used here. This energy density can be substituted into the energy integral, Eq. (6), and simplified with the same approximations that were used in Sec. 3.2 to find the anisotropy energy. Namely,

$$\begin{aligned} E_d &= 2\pi t \times \frac{\mu_0}{2} M_s^2 \cos^2 \Phi \int_0^\infty r \cdot \operatorname{sech}^2\left(\frac{R-r}{w}\right) dr \\ &\approx 2\pi t \times \mu_0 M_s^2 \cos^2 \Phi \times R w. && \text{(for } R \gg w\text{)} \end{aligned}$$

This result predicts that the demagnetising energy is similar to both DMI, in that it favours Bloch type skyrmions ($\cos \Phi = 0$), and to anisotropy, favouring small skyrmions.

3.4 Exchange

Neighbouring atomic spin sites in a ferromagnet have a tendency to align in the same direction, due to the exchange interaction. This is quantum mechanical in origin. Hence, there is an associated energy cost for gradients in the magnetisation. The energy density of the exchange interaction in bulk materials is given in cylindrical coordinates by (Aharoni 2000)

$$U_{ex} = A \left(\left(\frac{dm_r}{dr} \right)^2 + \left(\frac{dm_z}{dr} \right)^2 + \frac{m_r^2}{r^2} \right), \quad (13)$$

where A is the exchange stiffness, dependent upon the given material and the temperature. This can be substituted into the energy integral, Eq. (6), which is then approximately solved. Namely,

$$\begin{aligned} E_{ex} &= 2\pi t \times A \int_0^\infty \operatorname{sech}^2\left(\frac{R-r}{w}\right) \cdot \left(\frac{1}{w^2} + \frac{1}{r^2}\right) \cdot r \, dr \\ &\approx 2\pi t \times \frac{A}{w} \left(\frac{R}{w} + \frac{w}{R}\right) \int_0^\infty \operatorname{sech}^2\left(\frac{R-r}{w}\right) \, dr && \text{(for } R \gg w\text{)} \\ &\approx 2\pi t \times 2A \left(\frac{R}{w} + \frac{w}{R}\right). && \text{(for } R \gg w\text{)} \end{aligned}$$

The exchange energy is dependent on the ratio between the skyrmion's radius R and its wall width w . By inspection, this will be minimised when $R = w$. For skyrmions with a thin wall relative to the radius (large $\frac{R}{w}$), there is a sudden change in magnetisation, increasing the exchange energy. In the limit considered ($R \gg w$), the $\frac{w}{R}$ term will not grow and is far less significant than the $\frac{R}{w}$ term. Hence, the exchange energy favours skyrmions with a large wall width relative to its radius.

3.5 Zeeman Energy

In the presence of an external magnetic field, magnetic dipoles will have a tendency to align with this field, costing energy to deviate away. This is known as the Zeeman energy and its energy density is given by

$$U_{Zee} = -M_s B(m_z + 1), \quad (14)$$

where the externally applied magnetic field has a strength B in Tesla and acts in the positive z -direction. M_s is the magnetic saturation. The energy density can be substituted into the energy integral (6) to produce

$$\begin{aligned} E_{Zee} &= 2\pi t \times (-M_s B) \int_0^\infty r \times \left(\tanh\left(\frac{R-r}{w}\right) + 1\right) \, dr \\ &\approx 2\pi t \times (-M_s B) \left(R^2 + w^2 \int_0^\infty \frac{\rho}{1 + e^\rho} \, d\rho\right) && \text{(for } R \gg w\text{)} \\ &= 2\pi t \times (-M_s B) \left(R^2 + w^2 \frac{\pi^2}{12}\right). \end{aligned}$$

Because the external magnetic field acts in the same direction as the core of the skyrmion, the Zeeman energy favours large skyrmions. Our result supports this prediction, as the Zeeman energy is proportional to the area of the skyrmion πR^2 . Additionally, skyrmions with thicker walls have a larger area outside the skyrmion w^2 that is not misaligned against the external field.

4 Minimising Energy

With all the energy contributions expressed now as functions of R , w and Φ (skyrmion radius, wall width, and helicity), one can minimise the energy to find these quantities.

Each energy contribution can now be substituted into Eq. (3) resulting in the total energy

$$\begin{aligned}
 \frac{E_{total}}{2\pi t}(R, w, \Phi) &= -D \sin \Phi \times \pi R && \text{(DMI)} \\
 &+ 2KRw && \text{(Anisotropy)} \\
 &+ \mu_0 M_s^2 \cos^2 \Phi \times Rw && \text{(Demagnetising)} \\
 &+ 2A \left(\frac{R}{w} + \frac{w}{R} \right) && \text{(Exchange)} \\
 &- M_s B \left(R^2 + \frac{w^2 \pi^2}{12} \right). && \text{(Zeeman)}
 \end{aligned} \tag{15}$$

This is an analytic, approximate equation describing the total energy of a skyrmion in a bulk magnetic material.

4.1 Skyrmion Helicity

To begin characterising the skyrmion geometry, the values of skyrmion helicity Φ that minimise the total energy can be found by solving

$$\frac{\partial E_{total}}{\partial \Phi} = 0, \tag{16}$$

to find the stationary points. This leads to

$$-R \cos \Phi (2\mu_0 M_s^2 w \sin \Phi + \pi D) = 0,$$

which can be solved by considering each case, namely,

$$\begin{aligned}
 \cos \Phi = 0 & & \text{and} & & \sin \Phi = \frac{-\pi D}{2\mu_0 M_s^2 w} \\
 \Phi = -\frac{\pi}{2}, \frac{\pi}{2} & \quad (-\pi < \Phi \leq \pi) & & & \equiv d_{eff},
 \end{aligned} \tag{17}$$

where d_{eff} is defined as a unitless ratio of the DMI energy per unit area to the demagnetising energy per unit area of the skyrmion.

To determine the nature of these stationary points, the size of d_{eff} must be considered. When $|d_{eff}| \geq 1$, there are only two solutions to Eq. (16) so either the helicity $\Phi = -\frac{\pi}{2}$, or $\Phi = \frac{\pi}{2}$ is the local minimum, which are both Bloch-type skyrmions. This depends on the sign of d_{eff} , and hence the sign of the DMI strength D . When $|d_{eff}| < 1$, both $\Phi = -\frac{\pi}{2}$ and $\Phi = \frac{\pi}{2}$ are always local minima. $\Phi = \sin^{-1}(d_{eff})$ is always a local maximum and so can be disregarded.

These values for skyrmion helicity correspond with Bloch type skyrmions, which are commonly known to form in bulk magnetic materials (Camley & Livesey 2023). The two different helicities represent rotation in opposing directions. Therefore, different materials with different signs of D will favour skyrmions with different chiralities.

Substituting $\Phi = \frac{\pi}{2}$ into Eq. (15) gives

$$\frac{E_{total}}{2\pi t} = -D\pi R + 2KRw + 2A \left(\frac{R}{w} + \frac{w}{R} \right) + M_s B \left(R^2 + \frac{w^2 \pi^2}{12} \right), \tag{18}$$

which can be analysed to predict the radius and wall width.

4.2 Skyrmion Radius and Wall Width

To find the skyrmion radius, R , and wall width, w , that minimises the skyrmion energy, we must solve both

$$\frac{\partial E_{total}}{\partial R} = 0, \quad \frac{\partial E_{total}}{\partial w} = 0, \quad (19)$$

using Eq. (18). Setting the externally applied magnetic field to zero enables an analytic solution to be found. Simplifying Eqs. (19) with $B = 0$ leads to two quadratics of similar forms,

$$R^2 = \frac{2Aw^2}{2Kw^2 + 2A - \pi Dw}, \quad w^2 = \frac{2AR^2}{2KR^2 + 2A}. \quad (20)$$

By solving Eqs. (20) simultaneously, we find an analytic prediction for the skyrmion's wall width,

$$w = \frac{\pi D}{4K}, \quad (21)$$

and its radius,

$$R = \pi D \sqrt{\frac{A}{16AK^2 - \pi^2 KD^2}}. \quad (22)$$

Firstly, these results show the larger the DMI strength, D , the larger the skyrmion will be. Conversely, the stronger the anisotropy constant, K , the smaller the skyrmions will be. Additionally, there is a critical relationship between the DMI, anisotropy, and the exchange stiffness, A , for skyrmions to be stable. Namely,

$$|D| < \frac{4}{\pi} \sqrt{AK}. \quad (23)$$

Furthermore, the forms of both Eqs. (21) and (22) are similar to the existing predictions for skyrmions in thin-films (Lu et al. 2023).

5 Conclusion and Future Work

By assuming the skyrmion radius is significantly larger than the wall width, approximate expressions for the DMI, anisotropy, demagnetising, exchange and Zeeman energy contributions of a skyrmion were found for a bulk material. The total energy was then minimised to find analytic expressions for the helicity Φ , radius R , and wall width w . These are given in Eqs. (17), (21), and (22).

The next step in this work is to substitute real magnetic parameters into these analytic expressions to see if they accurately predict the geometry of skyrmions that have been experimentally measured. These parameters include the exchange stiffness A , saturation magnetisation M_s , anisotropy constant K and DMI strength D .

This research could be built upon by combining the interfacial DMI (presented in the literature, such as in Lu et al. (2023)) and the bulk DMI (derived here) energy contributions to form a comprehensive model of skyrmions in thick films. The helicity could also be researched further to investigate the potential bistable nature of skyrmion chirality.

So-called ‘‘intermediate skyrmions’’ with chirality $\Phi \sim \pi/4$ – between that of Bloch and Néel skyrmions – can also be found using our analytic model. These are of great interest currently as they can be pushed in a straight line for memory application (Dai et al. 2023). Bloch or Néel skyrmions instead have an issue of always moving in curved trajectories. This issue currently limits the technological use of skyrmions.

Acknowledgements

I wish to acknowledge the support and wisdom of my supervisor Karen Livesey. I certainly appreciate her mentoring of me that facilitated my involvement within this remarkable opportunity. I also acknowledge Python code provided by Ellen Lu, used to generate plots.

References

- Aharoni, A. (2000), *Introduction to the Theory of Ferromagnetism*, Vol. 109, Clarendon Press, Oxford.
- Camley, R. E. & Livesey, K. L. (2023), ‘Consequences of the Dzyaloshinskii-Moriya interaction’, *Surface Science Reports* **78**(3), 100605.
- Dai, B., Wu, D., Razavi, S. A., Xu, S., He, H., Shu, Q., Jackson, M., Mahfouzi, F., Huang, H., Pan, Q. et al. (2023), ‘Electric field manipulation of spin chirality and skyrmion dynamic’, *Science Advances* **9**(7), eade6836.
- Lu, E., Stuart, A. R., Chalifour, A. R., Davidson, J. C., Keatley, P. S., Buchanan, K. S. & Livesey, K. L. (2023), ‘Analytic theory for Néel skyrmion size, accounting for finite film thickness’, *Journal of Magnetism and Magnetic Materials* **584**, 171044.
- Tomasello, R., Martinez, E., Zivieri, R., Torres, L., Carpentieri, M. & Finocchio, G. (2014), ‘A strategy for the design of skyrmion racetrack memories’, *Scientific reports* **4**(1), 1–7.
- van Dijk, B. (2015), Skyrmions and the Dzyaloshinskii-Moriya interaction, Master’s thesis, Utrecht University.
- Wang, X., Yuan, H. & Wang, X. (2018), ‘A theory on skyrmion size’, *Communications Physics* **1**(1), 31.